Stem Cell Reports
Article

ISSCR

OPEN ACCESS

Parkin and PINK1 Patient iPSC-Derived Midbrain Dopamine Neurons Exhibit Mitochondrial Dysfunction and α-Synuclein Accumulation

Sun Young Chung,[1,2,11] Sarah Kishinevsky,[1,2,11] Joseph R. Mazzulli,[3] John Graziotto,[3] Ana Mrejeru,[4] Eugene V. Mosharov,[4] Lesly Puspita,[5] Parvin Valiulahi,[5] David Sulzer,[4,6,7] Teresa A. Milner,[8,9] Tony Taldone,[10] Dimitri Krainc,[3] Lorenz Studer,[1,2,*] and Jae-won Shim[5,*]

[1]Center for Stem Cell Biology, Sloan-Kettering Institute, New York, NY 10065, USA
[2]Developmental Biology Program, Sloan-Kettering Institute, Memorial Sloan-Kettering Cancer Center, 1275 York Avenue, Box 256, New York, NY 10065, USA
[3]Department of Neurology, Northwestern University Feinberg School of Medicine, Chicago, IL 60611, USA
[4]Department of Neurology, Columbia University Medical Center, New York, NY 10032, USA
[5]Soonchunhyang Institute of Medi-bio Science (SIMS), Soonchunhyang University, 25, Bongjeong-ro, Dongnam-gu, Cheonan-si 31151, Korea
[6]Department of Psychiatry
[7]Department of Pharmacology
Columbia University Medical Center, New York, NY 10032, USA
[8]Feil Family Brain and Mind Research Institute, Weill Cornell Medicine, New York, NY 10065, USA
[9]Harold and Margaret Milliken Hatch Laboratory of Neuroendocrinology, The Rockefeller University, New York, NY 10065, USA
[10]Molecular Pharmacology and Chemistry Program, Sloan-Kettering Institute, New York, NY 10065, USA
[11]Co-first author
*Correspondence: studerl@mskcc.org (L.S.), shimj@sch.ac.kr (J.-w.S.)
http://dx.doi.org/10.1016/j.stemcr.2016.08.012

SUMMARY

Parkinson's disease (PD) is characterized by the selective loss of dopamine neurons in the substantia nigra; however, the mechanism of neurodegeneration in PD remains unclear. A subset of familial PD is linked to mutations in *PARK2* and *PINK1*, which lead to dysfunctional mitochondria-related proteins Parkin and PINK1, suggesting that pathways implicated in these monogenic forms could play a more general role in PD. We demonstrate that the identification of disease-related phenotypes in PD-patient-specific induced pluripotent stem cell (iPSC)-derived midbrain dopamine (mDA) neurons depends on the type of differentiation protocol utilized. In a floor-plate-based but not a neural-rosette-based directed differentiation strategy, iPSC-derived mDA neurons recapitulate PD phenotypes, including pathogenic protein accumulation, cell-type-specific vulnerability, mitochondrial dysfunction, and abnormal neurotransmitter homeostasis. We propose that these form a pathogenic loop that contributes to disease. Our study illustrates the promise of iPSC technology for examining PD pathogenesis and identifying therapeutic targets.

INTRODUCTION

Parkinson's disease (PD) is the second most common neurodegenerative disorder and is characterized by the selective loss of midbrain dopamine (mDA) neurons in the substantia nigra (SN). While the majority of PD cases are sporadic, there has been considerable progress in the identification of genes related to familial forms of PD. The study of such rare mutations may illuminate novel strategies to predict, understand, and potentially treat PD. A number of PD animal models have been established, but most of these have failed to faithfully reproduce the human disease (Dawson et al., 2010). Recent advances in the derivation and differentiation of human induced pluripotent stem cells (iPSCs) and human embryonic stem cells (ESCs) present new opportunities for disease modeling (Bellin et al., 2012). The advent of iPSC technology has enabled PD modeling directly in patient-specific and disease-relevant human cells such as mDA neurons, the cell type preferentially lost in the disorder. To study mechanisms of mDA neuron loss in vitro, it is essential to select an optimized in vitro protocol to obtain the appropriate cell type. Many previous PD modeling studies in patient-specific iPSC lines were conducted using early generation differentiation protocols, which resulted in variable dopamine (DA) neuron populations in both quality and quantity (Cooper et al., 2012; Devine et al., 2011; Jiang et al., 2012; Nguyen et al., 2011). Therefore, the iPSC-derived DA neuron populations in those studies may have been heterogeneous and possibly distinct from the actual cells affected in the PD brain. We previously reported a successful protocol for deriving mDA neurons from human ESCs and iPSCs (Kriks et al., 2011), which facilitates robust induction of more "authentic" midbrain neurons that express key mDA markers including the transcription factors FOXA2 and LMX1A.

Patients with recessively inherited *PARK2*/Parkin (Kitada et al., 1998) and *PTEN-induced putative kinase 1* (*PINK1*) (Valente et al., 2004) mutations represent one of several monogenic forms of PD. Recent studies demonstrated the involvement of both Parkin and PINK1 in mitochondrial function (Imaizumi et al., 2012; Narendra et al., 2010; Seibler et al., 2011). In our study, we first used our floor-plate-based differentiation protocol to derive mDA neurons from

patient-specific *PINK1* and *PARK2*/Parkin mutant human iPSCs. The PD iPSC lines displayed differentiation properties comparable with those of control human iPSC or ESC (H9) lines; however, both PINK1 and Parkin patient-derived mDA neurons showed increased levels of α-synuclein expression at the gene and protein levels. The PD iPSC-derived mDA neurons also exhibited increased susceptibility to mitochondrial toxins. Furthermore, we found mitochondrial abnormalities and increased intracellular DA levels in floor-plate-derived PD iPSC mDA neurons. On the contrary, DA neurons generated via a neural rosette/neuroepithelial (Perrier et al., 2004) rather than via a floor-plate intermediate (Kriks et al., 2011) did not show a difference in phenotypes including α-synuclein levels between disease and control lines. Our findings highlight the importance of the appropriate mDA neuron identity for in vitro disease modeling and point to a pathogenic loop that includes mitochondrial dysfunction, increased vulnerability, and the accumulation of α-synuclein and dopamine.

RESULTS

Characterization of Differentiation Potential of PD iPSCs

We analyzed two iPSC lines derived from patients with *PARK2*/Parkin (V324A) and *PINK1* (Q456X) mutations, lines established and studied in past reports (Cooper et al., 2012; Mazzulli et al., 2011, 2016; Miller et al., 2013; Seibler et al., 2011). For this study, we used our previously published midbrain floor-plate-based mDA neuron differentiation protocol (Kriks et al., 2011) to differentiate the Parkin and PINK1 iPSC as well as control human iPSC and ESC lines. The mDA neuron protocol is based on neural induction via dual-SMAD inhibition (Chambers et al., 2009) and the sequential activation of SHH and WNT signaling (Kriks et al., 2011). Disease and control lines were differentiated simultaneously to assess the efficiency of mDA neuron yield (Figure 1). At day 11 of differentiation, all lines demonstrated a high yield (70%–90%) of midbrain precursor cells co-expressing FOXA2 and LMX1A, which are critical markers in mDA neuron development (Figures 1A and 1B). At day 30 cells began to express tyrosine hydroxylase (TH), the rate-limiting enzyme in the production of DA, which was co-expressed with the midbrain-related transcription factors FOXA2 and NURR1 (Figures 1C and 1D). Upon further maturation, cells maintained high levels of FOXA2/NURR1 and continued to express TH (Figures 1E and 1F). DA neurons from all lines demonstrated co-expression with MAP2, a marker of post-mitotic neurons (Figure S1A).

Moreover, DA neurons derived from PD or control iPSCs lines demonstrated comparable yields of FOXA2, NURR1, and TH, suggesting suitability for in vitro PD modeling. In contrast, DA neurons derived using the stromal feeder (MS5)-based differentiation protocol (Perrier et al., 2004), whereby cells transit through a neural rosette stage rather than a floor-plate intermediate, yielded significantly lower levels (20%–50%) of TH^+ neurons (Figures 1G and 1H). The transcription factors FOXA2/NURR1 were expressed in only a small proportion of the total cell population, and cells expressing these markers often did not co-express TH. Electrophysiological recordings of H9, control iPSC, and PD iPSC-derived (day 80) DA neurons demonstrated that the floor-plate-based protocol yields cells with slow oscillatory action potentials at 3–5 Hz, at a resting membrane potential of −45 mV (n = 12 cells). This spontaneous tonic firing activity is another prominent characteristic of mDA neurons, including those located in the substantia nigra pars compacta (SNpc) (Figures S2A–S2D). These data confirm that floor-plate-derived but not neural-rosette-derived TH^+ neurons exhibit marker expression and functional properties characteristic of midbrain-specific DA neurons.

Mitochondrial Defects in Differentiated Cells from PD iPSCs

Parkin and PINK1 proteins are thought to play important roles in mitochondrial homeostasis, based on studies in which increased expression of those genes confers protection from stress-induced cell death. Furthermore, loss of Parkin and PINK1 makes primary cells more susceptible to stress and death (Deng et al., 2008; Exner et al., 2007; Poole et al., 2008; Valente et al., 2004). Based on such results, it is believed that *PARK2*/Parkin- and *PINK1*-related genetic causes of PD likely involve a loss-of-function phenotype that leads to the clinical presentation of the disease (Klein and Schlossmacher, 2006; Lesage and Brice, 2009). To gain a better understanding of the Parkin- and PINK1-mediated PD phenotype, we investigated the presence of mitochondrial abnormalities that have been described in DA neurons of PD patients and neuronal cultures (Devi et al., 2008; Imaizumi et al., 2012; Keeney et al., 2006; Pickrell and Youle, 2008). For both Parkin- and PINK1 iPSC-derived midbrain neuronal populations, electron microscopy at day 75 of differentiation revealed the presence of abnormal mitochondria (Figure 2A). The PD iPSC-derived neuronal populations had a greater proportion of enlarged mitochondria (60%–80% of mitochondria), a finding observed in a much smaller fraction of control iPSC- or ESC-derived neurons (Figure 2B) Abnormal mitochondria were also larger (60%–120%) than those in neurons derived from control iPSC or ESC (H9) lines (Figure 2C). Neurons

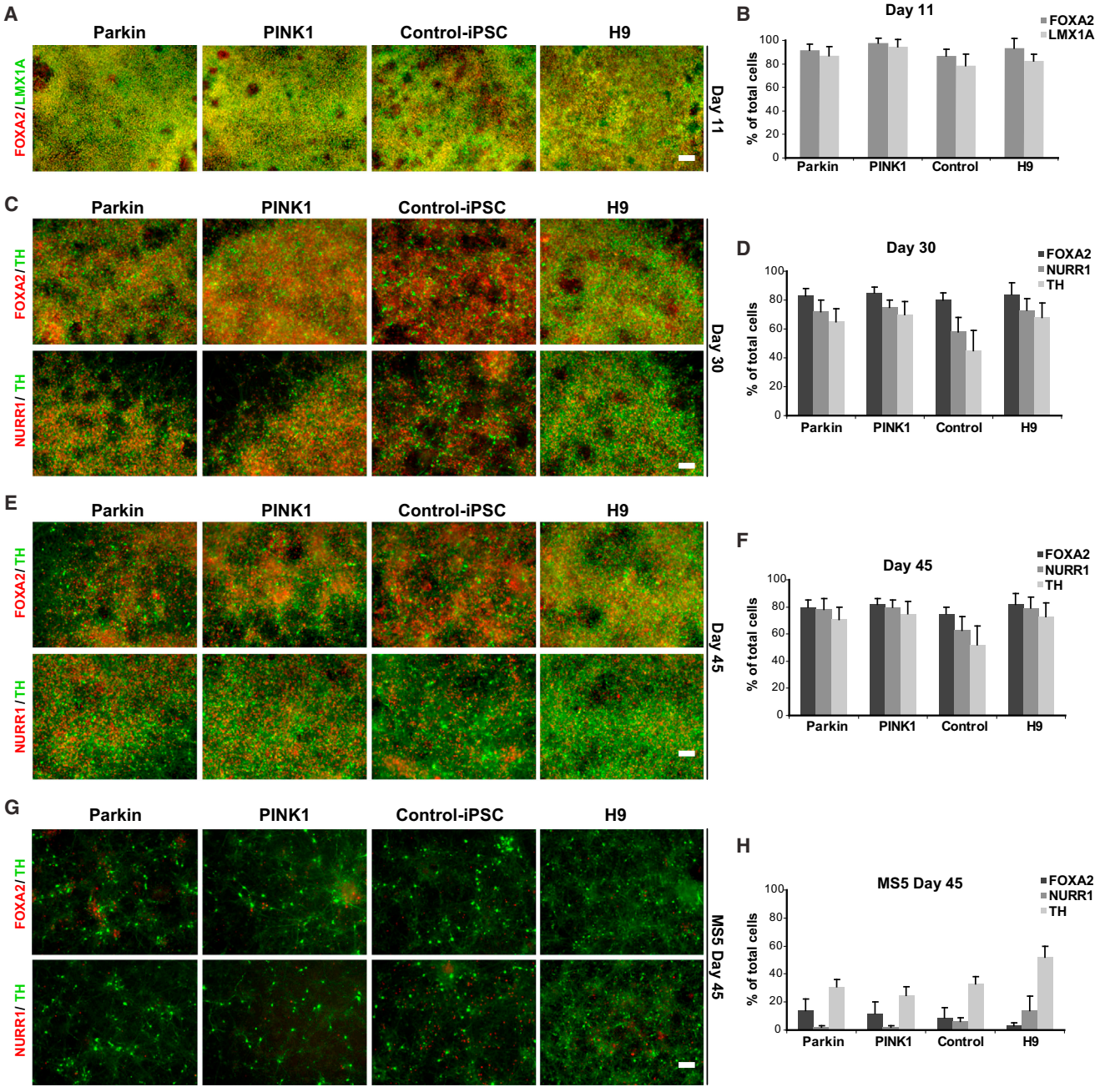

Figure 1. Identical Differentiation Potential of PD iPSC and Control Lines

(A, C, E, and G) Immunocytochemical analysis of in-vitro-derived mDA neuron lineages at day 11 (A; midbrain precursor stage), day 30 (C; early post-mitotic neuronal stage), and day 45 (E and G; mature neuronal stage) of differentiation. FOXA2, LMX1A, NURR1, and TH expression was assessed in Parkin and PINK1 iPSC lines, control iPSC, and normal ESC (H9) lines. Representative images in (A), (C), and (E) illustrate mDA neuron cultures differentiated by the floor-plate-based protocol. Images in (G) illustrate cells differentiated via the MS5-based protocol. Scale bars, 50 μm.

(B, D, F, and H) Quantification of the data are presented in (A), (C), (E), and (G), respectively.

All data are presented as mean ± SEM. See also Figures S1 and S2.

generated from the MS5-based differentiation protocol were imaged at day 50 of differentiation and, unlike in those generated from the floor-plate-based protocol, there were no significant differences in mitochondrial size and morphology between control and patient lines (Figures S3A–S3C).

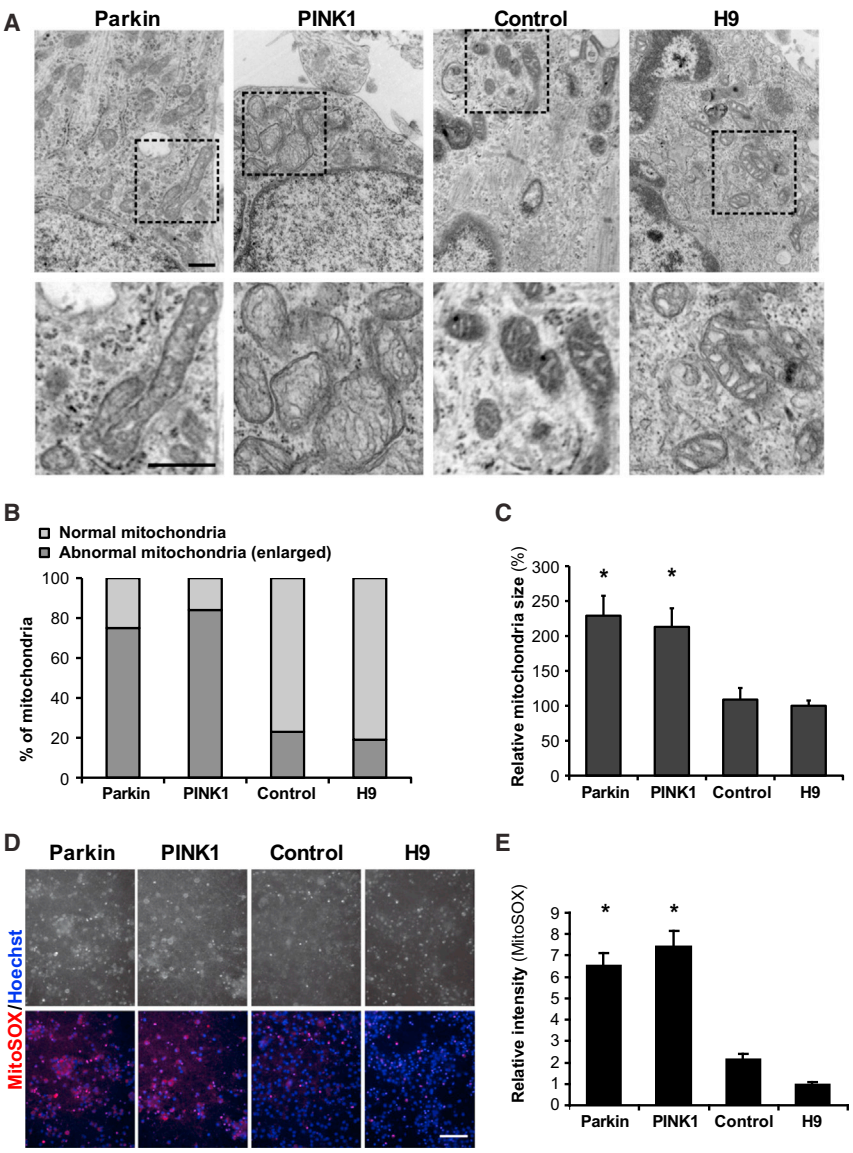

Figure 2. Abnormal Mitochondria in PD iPSC-Derived Midbrain Neuronal Population

(A) Electron microscopy photographs taken at day 75 of differentiation. Lower panels are enlarged images of the corresponding boxed area marked in upper panels. Scale bar, 500 nm.

(B) Percentage of abnormally shaped mitochondria among all mitochondria in a given midbrain neuronal population.

(C) Relative mitochondria size for each line compared with the average size measured in H9-derived cells (n = 20–50; mitochondria from two independent preparations). Significance levels for individual markers are presented as comparisons with the H9 wild-type group: *p < 0.01, ANOVA and Dunnett's test.

(D) Live staining image of MitoSOX indicating oxidative mitochondria. Black and white images in the upper panels and red color in the lower panels represent MitoSOX labeling, and blue (lower panels) represents Hoechst for DNA. Scale bar, 50 μm.

(E) Quantification of relative fluorescence intensity of MitoSOX by image analysis (n = 3; independent experiments). Significance levels for individual markers are presented as comparisons with the H9 wild-type group: *p < 0.001, ANOVA and Dunnett's test. All data are presented as mean ± SEM. See also Figure S3.

Mitochondrial Stress and Cell-Type-Specific Vulnerability in mDA Neurons

To explore functional changes associated with the gross phenotypic abnormalities in the mitochondria, we measured mitochondrial-derived oxidants with the MitoSOX assay (Figures 2D and 2E) as a readout of mitochondrial stress. PD iPSC-derived mDA cells displayed MitoSOX-positive mitochondria widely distributed throughout the cytosol (Figure 2D). In contrast, the relative MitoSOX intensity in control iPSC and wild-type ESC mDA populations was much lower than that of patient neurons (Figure 2E) and mainly confined to apoptotic, shrunken cells (Figure 2D). The apparent mitochondrial phenotype in our PD iPSC-derived mDA neurons and the nature of the primary genetic defect suggest that mitochondrial dysfunction is likely a driving factor responsible for a variety of downstream phenotypes.

Next, we investigated whether PINK1 or Parkin iPSC-derived cells were prone to cell death, since progressive degeneration of DA neurons in the SN is a prominent feature of PD. Under standard culture conditions we did not observe a noticeable difference in mDA neuron survival between PD and control lines (Figure 3A, upper panels). To determine whether PD lines are sensitive to mitochondrial stress, we used CCCP (carbonyl cyanide m-chlorophenyl hydrazone), a chemical inhibitor of oxidative phosphorylation and potential mitochondrial stress inducer, to explore differences in cell survival (Figure 3A, lower panels). Cells at days 60–70 of differentiation were treated with increasing concentrations of CCCP for 48 or 72 hr,

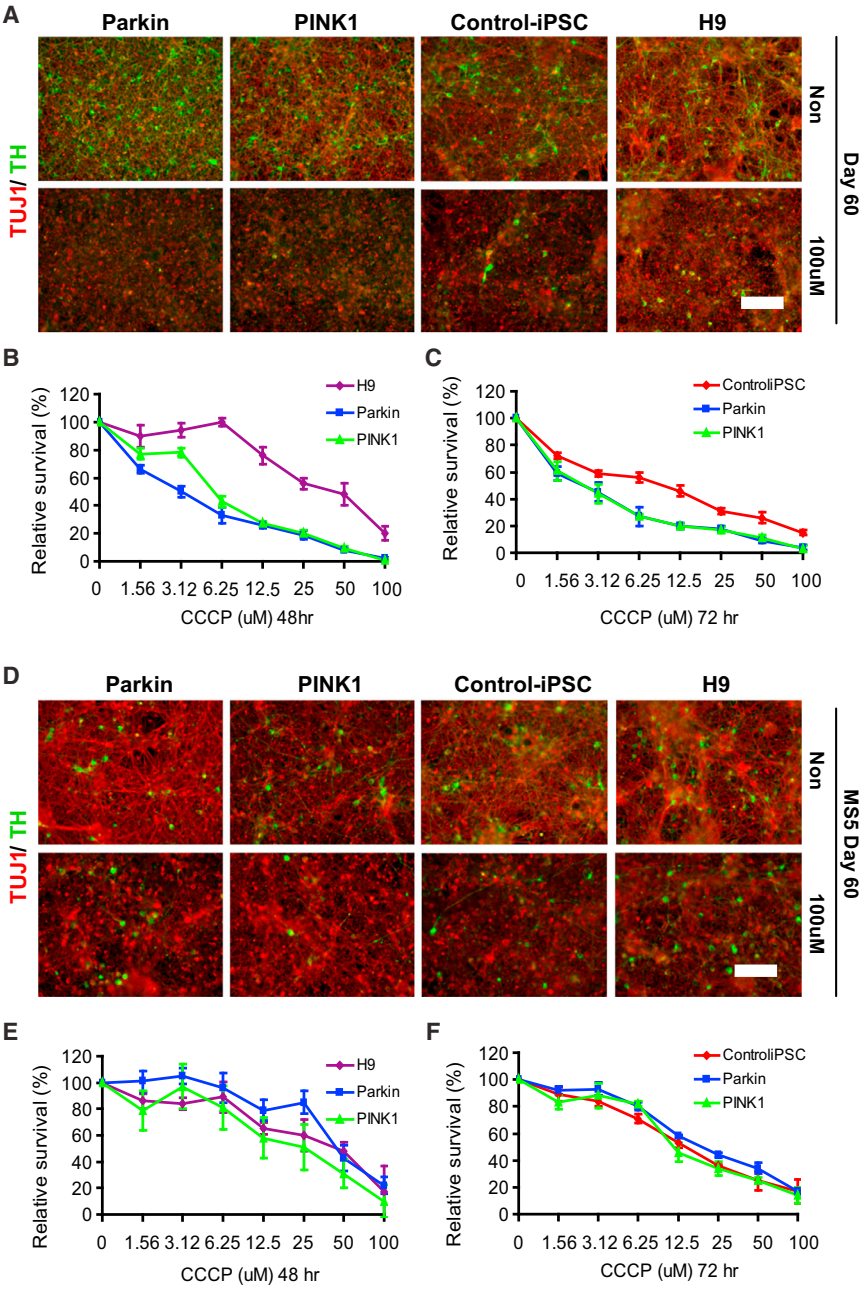

Figure 3. Vulnerability to Mitochondria Toxin

(A and D) Immunocytochemical analysis at day 60 in mDA neurons derived via the floor-plate-based protocol (A) or MS5 feeder-based protocol (D) for TUJ1 and TH: treatment with 100 μM CCCP. Scale bars, 50 μm. (B, C, E, and F) Cell-viability assay with ATP activity after 48 or 72 hr of CCCP treatment (day 60 of differentiation of floor-plate-based protocol [B and C] and MS5 feeder-based protocol [E and F], three technical replicates).

All data are presented as mean ± SEM.

and cell survival was analyzed using an ATP activity assay. The results revealed that differentiated mDA cells from either of the two PD iPSC lines were more vulnerable than those derived from control iPSC or ESC lines (Figures 3B and 3C). Our data support previous studies (Nguyen et al., 2011; Shaltouki et al., 2015) suggesting that PD iPSC-derived mDA neurons are more susceptible to cell stress and death. This is compatible with clinical observations noting elevated vulnerability of PD patient DA neurons to cell death due to stressors such as oxidative damage, nitrosative damage, and environmental toxins (Hauser and Hastings, 2013). Of note, DA populations derived from the MS5 feeder-based protocol did not exhibit any differences in vulnerability to CCCP between PD iPSCs and control lines (Figures 3D–3F).

α-Synuclein Accumulation in PD iPSC-Derived mDA Neurons

α-Synuclein is a natively unfolded, presynaptic neuronal protein strongly implicated in PD and Alzheimer's disease,

and other neurodegenerative disorders (Arima et al., 1998). Mutations in the *SNCA* gene or abnormalities in α-synuclein expression and regulation (Abeliovich et al., 2000; Bellucci et al., 2012) are thought to be actively involved in mDA neuron degeneration and PD pathogenesis. In particular, aggregation of α-synuclein protein is a key feature of Lewy bodies, neuronal inclusions that are a pathological hallmark of PD. Although the role of α-synuclein has yet to be fully elucidated, evidence indicates it plays an important role in the regulation of various neuron-related mechanisms such as vesicle transport and synaptic vesicle fusion (Abeliovich et al., 2000; Bendor et al., 2013). In the context of PD, studies suggest that abnormal aggregation of α-synuclein can be induced by oxidative stress (Norris et al., 2007; Paxinou et al., 2001; Sherer et al., 2002), and the presence of oxidized/nitrated α-synuclein has also been documented in the PD brain (Giasson et al., 2000). Therefore, we assessed whether α-synuclein pathology can be observed in vitro in PD iPSC-derived DA neurons. Quantitative immunocytochemistry and RT-PCR analyses revealed a progressive increase in α-synuclein expression during mDA neuron differentiation and maturation (Figures 4A–4H). However, at the level of gene expression, we did not observe obvious differences between control- and PD iPSC-derived cells (Figure 4E). Expression of α-synuclein by immunocytochemistry was detected starting at day 45 of differentiation in mDA neurons derived from PD iPSC lines (Figures 4A–4C and 4F). By day 60, α-synuclein was abundantly expressed across all groups, but higher in PD than in control iPSC lines. In addition, PD iPSC-derived neurons showed increased cytoplasmic localization of α-synuclein, which was present in a higher proportion of TH^+ neurons compared with control iPSC- or ESC-derived mDA neurons (Figures 4C and 4G). In MS5-derived (non-floor-plate) cultures, the percentage of TH^+ cells expressing α-synuclein was lower than in floor-plate-derived cultures, and no differences were observed between PD iPSC and control-derived cells (Figures 4D and 4H). Using the floor-plate protocol, differences in α-synuclein levels between PD iPSC and control groups were further corroborated by western blotting analysis showing elevations in Triton-soluble extracts of PD iPSC neurons (Figures 5A and 5C). Measurement of neuronal markers including βIII-tubulin and MAP2 indicated that control and patient lines differentiated into neurons similarly, suggesting that α-synuclein accumulation occurred as a pathological process rather than representing a maturation-related difference (Figure 5B). To further address this issue, we analyzed the levels of tau expression, another maturation-related marker and a protein prone to aggregation. Western blotting for tau revealed no change in levels between control and patient lines, indicating a comparable maturation state, confirming the specificity of α-synuclein accumulation in the PINK1 and Parkin patient lines (Figure 5B). We next measured the specific accumulation of pathological α-synuclein in patient lines by analyzing Triton-insoluble extracts by western blot using the α-synuclein antibody LB509, which was generated against Lewy body inclusions (Baba et al., 1998). Elevated levels of insoluble α-synuclein were detected in patient lines with LB509, and confirmed with another α-synuclein antibody, C20 (Figure 5C). Similar biochemical analysis of pathogenic α-synuclein was performed in MS5-derived neurons, but no changes between disease and control lines were observed (Figures S4A–S4D). Immunocytochemical analysis revealed that α-synuclein-positive cells co-expressed ubiquitin (Figure S5A), another protein found in Lewy bodies (Engelender, 2008); however, we did not observe significant differences in the levels of total ubiquitin between disease and control lines (Figure S5B), which may be due to the fact that ubiquitin expression can be regulated independently of α-synuclein levels. To determine whether increased α-synuclein levels in PD iPSC lines resulted from mutant *PINK1*, we overexpressed wild-type *PINK1* gene via lentiviral transduction at day 35 of differentiation. At day 53, cells transduced with the *PINK1* rescue vector showed a partial reduction in α-synuclein expression compared with non-transduced cells and cells transduced with a control vector (Figures S6A and S6B). These data suggest a possible direct link between α-synuclein accumulation and the underlying genetic abnormality. We further tried to rescue α-synuclein accumulation by pharmacological means using superoxide dismutase (SOD) mimetics (MnTBAT and EUK134 [10–100 μM]) and N-acetyl-L-cysteine (1–10 mM), a powerful antioxidant (differentiation day 40–60); however, these pharmacological interventions did not yield significant differences in α-synuclein levels (data not shown).

Upregulation of Cytosolic Dopamine and Synapsin Levels

Our data demonstrate a correlation between mitochondrial dysfunction, elevated α-synuclein levels, and greater vulnerability to CCCP. We hypothesized that increased α-synuclein levels may also be associated with elevated cytosolic DA, as previous studies suggest that α-synuclein regulates DA transmission in DA neurons (Bendor et al., 2013; Mosharov et al., 2009). To address this question, we compared the levels of DA in mDA neurons derived from PD iPSC and control lines. Using high-performance liquid chromatography (HPLC) analysis with electrochemical detection, we observed elevated levels of intracellular DA in Parkin iPSC-derived mDA neurons (Figure 5D). Higher DA levels may point to hyperactive neurotransmitter biosynthesis, an increased number of storage or synaptic vesicles, or decreased DA metabolism. Intracellular DA

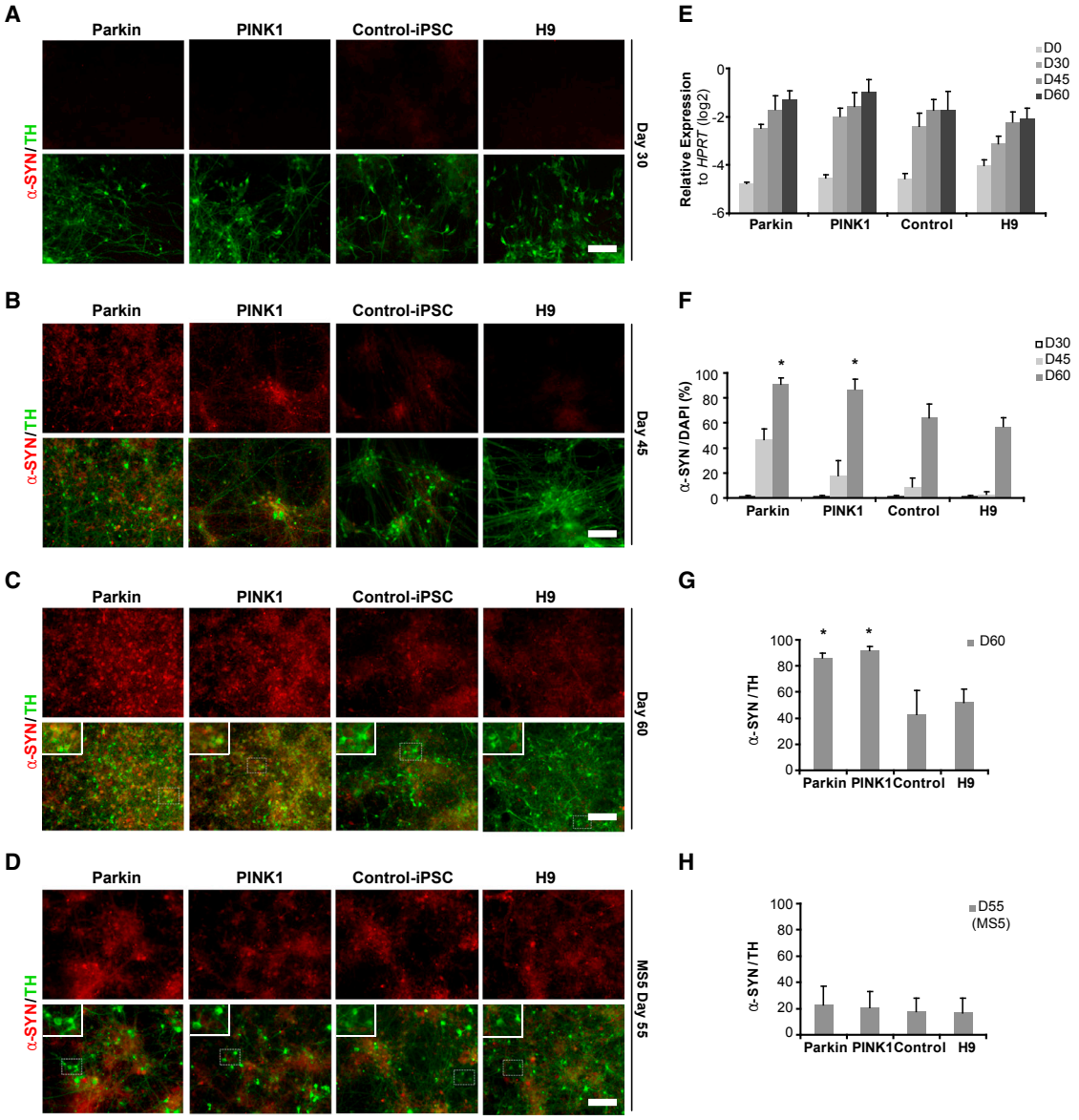

Figure 4. Difference in α-Synuclein Accumulation between PD iPSC and Control Lines

(A–D) Immunocytochemical analysis at days 30, 45, and 60 of differentiation for α-synuclein and TH expression from Parkin and PINK1 iPSC lines, control iPSC, and normal ESC (H9) lines. Panels in (A–C) show cells differentiated via the floor-plate-based protocol while panels in (D) were differentiated via the MS5 feeder-based protocol. Scale bars, 50 μm.

(E) RNA expression of *SCNA* (α-synuclein) at differentiation days 0, 30, 45, and 60 of each line (n = 9; technical replicates from three independent experiments).

(F) Quantification of the α-synuclein expression levels presented in (A–C) (n = 3; independent experiments).

(G and H) Quantitative co-expression analysis of α-synuclein and TH at day 60 of differentiation for the floor-plate-based protocol (C) and MS5 feeder-based protocol (D) (n = 3; independent experiments). Significance levels for individual markers are presented as comparisons with the H9 wild-type group: *p < 0.001, ANOVA and Dunnett's test.

All data are presented as mean ± SEM. See also Figures S5 and S6.

levels in neurons derived from MS5-based differentiations were also measured, but there were no significant differences between control and patient lines (Figure S4E). While further studies are required to address this question, we observed preliminary evidence of increased synapsin in Parkin iPSC-derived DA neurons (Figure 5A). This is compatible with a recent study that demonstrated interaction between synapsin III and α-synuclein in mice (Zaltieri et al., 2015).

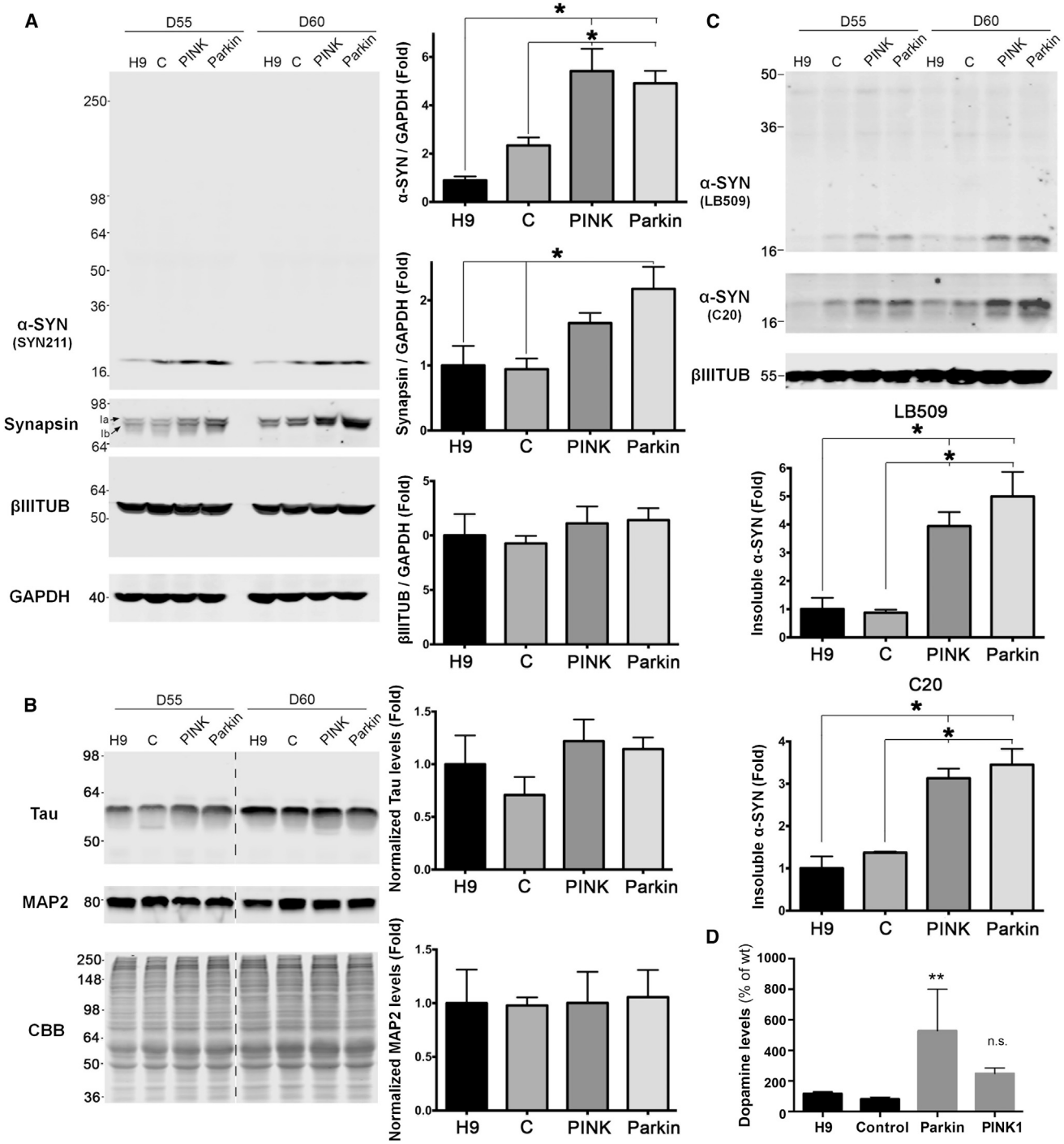

Figure 5. Accumulation of α-Synuclein and DA from PD iPSC-Derived mDA Population

(A) α-Synuclein and synapsin western blot analysis of Triton-soluble extracts from day-55 or day-60 mDA cultures. βIII-Tubulin and GAPDH were used as loading controls. For all blots, molecular weight is shown in kDa. Right: α-synuclein, βIII-tubulin, and synapsin were quantified and normalized to GAPDH. Data are expressed as fold change compared with the H9 line (n = 3; independent experiments). C, control iPSC line. Significance levels for individual markers are presented as comparisons with the H9 wild-type group or the control iPSC group: *p < 0.05, ANOVA and Tukey's multiple comparison test.

(legend continued on next page)

DISCUSSION

Our study reports several PD-associated phenotypes in mDA neurons derived from Parkin and PINK1 iPSCs. We focused on these two genetic forms of PD, which have been implicated in a variety of cellular functions including vesicular trafficking and mitochondrial maintenance (Pickrell and Youle, 2008). The fact that several disease-related phenotypes such as mitochondrial morphology, as well as levels of α-synuclein and cytosolic DA, were observed only in mDA neurons derived via the floor-plate protocol (Kriks et al., 2011) but not in cultures differentiated via a neuroepithelial intermediate on MS5 feeder cells suggests that the differentiation paradigm can greatly affect the outcome in PD iPSC-based in vitro modeling studies. Other recent PD iPSC-based disease modeling studies have utilized differentiation protocols with TH^+ neuron yields ranging from 10% to 15% (Nguyen et al., 2011; Shaltouki et al., 2015) and subtype characterization of those TH^+ cells often remains incomplete. The current study was focused on defining multiple PD-related disease phenotypes within a limited set of well-characterized iPSC lines and on determining the impact of distinct differentiation protocols within a given disease line. However, it will be important to confirm our results across a larger set of PD iPSC lines in the future.

It is noteworthy that while α-synuclein (*SNCA*) gene expression was unchanged across cell lines, immunostaining provided evidence of α-synuclein accumulation localized to the cytosol in the PD iPSC lines. It is well known that α-synuclein can exist in several different forms (Marques and Outeiro, 2012). Studies point toward the oligomeric and fibrillary α-synuclein species as being the toxic and pathogenic forms present in Parkinson's disease while the monomeric or tetrameric α-synuclein are likely physiological forms (Bartels et al., 2011; Marques and Outeiro, 2012). Future research should address whether in addition to increased protein levels and changes in α-synuclein cytoplasmic localization, PD iPSC-derived mDA neurons also exhibit changes in the ratio of oligomeric and fibrillary species. Interestingly, our results on the expression of α-synuclein in Parkin iPSC-derived mDA neurons are distinct from those of a previous study (Jiang et al., 2012), which reported no differences between disease and wild-type lines, but coincident with findings of partially upregulated α-synuclein in a subset of Parkin patient PD lines (Imaizumi et al., 2012). Evidence of α-synuclein accumulation is particularly intriguing for *PARK2*/Parkin mutant cells as many patients, particularly those carrying heterozygous mutations (Farrer et al., 2001), lack Lewy bodies at autopsy. In the study by Imaizumi et al. (2012), α-synuclein accumulation was observed in iPSC-derived DA neurons from a homozygous patient with a deletion in exons 2–3 but not in cells from another homozygous Parkin patient with deletions in exons 6 and 7. These results correlated with the presence or absence of Lewy bodies in autopsy data from the matched patient or family member. The Parkin iPSC line in our study was derived from a patient with a homozygous deletion in exon 9 with unknown patient pathology. A factor that may explain the presence or absence of α-synuclein accumulation in iPSC-derived DA neuron cultures is the specific differentiation protocol used. This is illustrated in our study by the absence of α-synuclein accumulation in MS5-derived cultures. Additional studies are required to further explore the mechanisms involved in the differences in α-synuclein levels across DA neuron protocols and *PARK2*/Parkin genotypes.

In addition, we observed significantly elevated levels of synapsin and dopamine in Parkin cultures, although the changes in PINK1 cells did not reach statistical significance when compared with control iPSC- or ESC-derived floor-plate mDA neurons. Increased DA levels may appear, in contrast to the well-known loss of DA in the brain of PD patients. While reduction in the PD brain may simply reflect the progressive loss of DA-producing neurons, there are data suggesting a reduction in DA levels or release in the remaining cells (Nguyen et al., 2011). Our HPLC data argue for an increase in intracellular dopamine levels in PD versus control iPSC-derived mDA neurons, which may be indicative of dysregulation of neurotransmitter release linked to

(B) Western blot analysis for MAP2C and tau. Coomassie brilliant blue (CBB) was used as a loading control. For all blots, molecular weight is shown in kDa. Right: quantification of tau and MAP2c indicate similar neuralization between control and patient lines (n = 3; independent experiments). The dashed line indicates cropped-out replicates, but all samples were run on the same gel.
(C) Western blot analysis of Triton-insoluble α-synuclein using antibodies LB509 and C20. For all blots, molecular weight is shown in kDa. Lower panels: quantification of insoluble α-synuclein, normalized to βIII-tubulin (n = 3; independent experiments). Significance levels for individual markers are presented as comparisons with the H9 wild-type group or the control iPSC group: *p < 0.05, ANOVA and Tukey's multiple comparison test.
(D) HPLC analysis for intracellular DA level at differentiation day 90 from Parkin and PINK1 iPSC lines, control iPSC line, and normal ESC (H9) line (n = 6; independent experiments). Significance levels for DA measured in Parkin or PINK1-derived mDA neurons are presented as comparisons with those measured in control mDA neurons (H9 and wild-type iPSC groups) by ANOVA and Dunnett's multiple comparison test: **p < 0.01; n.s., not significant.
All data are presented as mean ± SEM. See also Figure S4.

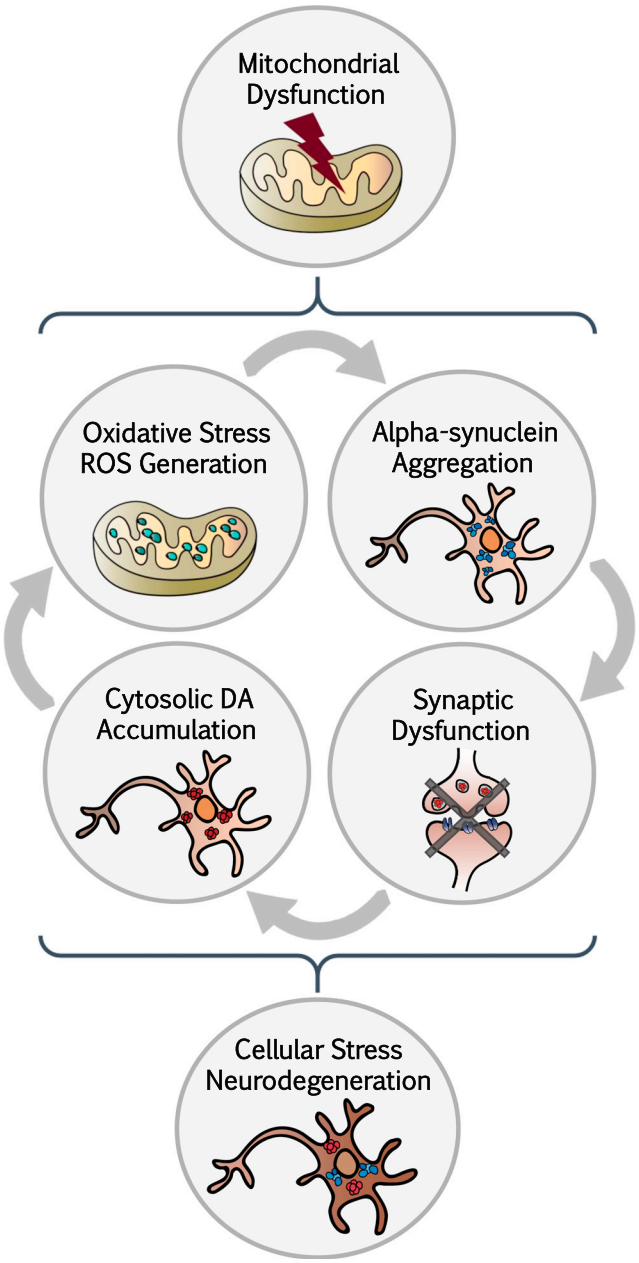

Figure 6. Proposed Model of the Pathogenic Loop in Parkin- and PINK1-Derived mDA Neurons

Mutations in *PARK2*/Parkin and *PINK1* at the origin of the disease phenotype trigger changes in mitochondrial homeostasis, which initiate multiple pathogenic changes throughout the cell. Dysregulation in various cellular functions ultimately induces cell-type-specific toxic cues, degeneration, and cell death in mDA neurons. ROS, reactive oxygen species.

changes in synaptic activity. In support of our findings, previous animal studies have also reported increased levels of DA and DOPAC in Parkin- and PINK1-deficient mice (Kitada et al., 1998). Alternatively, this could be due to a loss of ATP and the proton gradient, which determines the synaptic vesicle-to-cytosol equilibrium of DA. It will be important to address whether such changes are limited to the Parkin, or potentially, the PINK1 phenotype or reflect changes in other genetic or sporadic forms of PD at distinct stages of disease. It is tempting to speculate whether increased levels could contribute to the pathogenic cycle induced by mitochondrial dysfunction and ultimately lead to mDA neuronal cell death (Figure 6).

Determining the role of α-synuclein in PD pathogenesis is complicated by the fact that the physiological role of α-synuclein is not fully known; nevertheless, studies have linked α-synuclein to a variety of functions including the regulation of synaptic membrane processes and regulation of neurotransmitter release (Davidson et al., 1998; Nemani et al., 2010). Notably, α-synuclein has also been found to act as a negative regulator of synaptic vesicle fusion and exocytotic DA release, and studies have found that its overexpression impairs DA transmission in the early phases of neurodegeneration (Gaugler et al., 2012; Platt et al., 2012). Along these lines, other groups have found that absent or mutated α-synuclein can affect the compartmentalization of presynaptic DA and alter DA storage-pool capacity (Abeliovich et al., 2000; Mosharov et al., 2006; Murphy et al., 2000; Yavich et al., 2004). Furthermore, phage display and nuclear magnetic resonance spectroscopy have revealed that synapsin Ia is a binding partner of α-synuclein, which suggests that their interaction may play a critical role in the release of neurotransmitters (Woods et al., 2007). These results indicate that increased intracellular levels of DA observed in PD iPSC mDA neurons could be related to vesicular trafficking defects caused by α-synuclein protein dysfunction and other synaptic changes. Increased reactive oxygen species (ROS) resulting from defective mitochondria in PD mDA neurons may trigger destruction of synaptic vesicles, disrupt proper encapsulation of DA within vesicles, and cause the loss of the proton gradient required for synaptic vesicles to accumulate DA against its concentration gradient. Such abnormal DA homeostasis could eventually perpetuate a cascade of oxidative stress within already vulnerable cells.

In conclusion, our study illustrates the utility of the floor-plate-based mDA neuronal differentiation protocol for modeling aspects of PD in patient-specific cells. The results indicate that the identity of iPSC-derived mDA neurons is a critical factor in defining disease-relevant phenotypes for in vitro models. Our data further suggest a pathogenic loop involving mitochondrial dysfunction, elevated α-synuclein, synaptic dysfunction, DA accumulation, and increased oxidative stress and ROS. Studies will be required in the future to test this model using alternative strategies and to define whether similar mechanisms are involved

in other genetic or sporadic forms of PD and relevant neurodegenerative disorders.

EXPERIMENTAL PROCEDURES

Culture of Undifferentiated ESCs and iPSCs Including PD Patient iPSCs

PD iPSCs generated by retroviral overexpression of *OCT4*, *SOX2*, *KLF4*, and *C-MYC* from patients with mutations in *PARK2*/Parkin (B125 line) or *PINK1* (L2122 line) were generously provided by the D. Krainc laboratory (Northwestern University Feinberg School of Medicine). Information about patients and familial control is provided in Table S1. ESC lines H9 (WA-09, passages 35–45) and iPSC lines B125 (passages 20–30; *PARK2*/Parkin mutated line), L2122 (passages 20–30; *PINK1* mutated line), and L2131 and L2135 (passages 20–30; familial controls of *PINK1* mutated patient) were maintained on mouse embryonic fibroblasts (Global Stem) in 20% knockout serum replacement (Invitrogen)-containing human ESC medium as described previously (Kim et al., 2011). This study had been reviewed by the Tri-SCI ESCRO Committee (protocol number 2010-09-001).

Neuronal Differentiation

For FP-based mDA neuron induction, a modified version of the dual-SMAD inhibition was used based on our previously described differentiation protocol (Kriks et al., 2011). For rosette-based DA neuron induction we followed our previously described protocols (Perrier et al., 2004) but used dual-SMAD inhibition to accelerate the initial neural induction step. See Supplemental Experimental Procedures for details of the protocol.

Immunocytochemistry

Cells were fixed in 4% paraformaldehyde and blocked with 1% BSA with 0.3% Triton X-100. Primary antibodies were diluted in 1%–5% BSA and incubated according to the manufacturer's recommendations. A comprehensive list of antibodies and sources is provided in Table S2. Appropriate Alexa Fluor 488-, 555-, or 647-conjugated secondary antibodies (Molecular Probes) were used with DAPI nuclear counterstain (Thermo Fisher).

Electrophysiology

Whole-cell current-clamp recordings were performed. See Supplemental Experimental Procedures for detailed recording conditions.

Electron Microscopy

All steps were conducted as previously described (Milner et al., 2011). See Supplemental Experimental Procedures for procedural details. Cell morphology and organelles were identified using standard criteria (Peters et al., 1991). We assessed 20–50 mitochondria (n) in each group randomly selected from 10–20 images (approximately 250 μm^2 from Parkin iPSC, 600 μm^2 from PINK1 iPSC, 450 μm^2 from control iPSC, and 500 μm^2 from H9 ESC). Samples were prepared from two independent preparations. Abnormal mitochondria were identified based on enlarged length (elongated) or size (swollen). To be counted as abnormal in length or size, mitochondria needed to show a change of >1.5-fold above the respective average values in matched H9 ESC-derived cultures.

Mitochondrial ROS Assessment

Cells were stained with MitoSOX Red mitochondrial superoxide indicator (Life Technologies) at a final concentration of 20 μM in cell-culture medium. Staining was carried out in a 37°C incubator for 30 min. Hoechst dye was used for counterstaining. Quantification of the fluorescence intensity that oxidized the MitoSOX reagent was performed with ImageJ (NIH) and averaged for three independent experiments.

Cell-Viability Assay

To measure cell vulnerability against stress, we administered 1.56, 3.12, 6.25, 12.5, 25, 50, and 100 μM CCCP (Sigma) to differentiated cell populations of days 60–70 from each line. After 48 or 72 hr of treatment, cell survival was measured with CellTiter-Glo Luminescent Cell Viability Assay (Promega) with three technical replicates. Luminescent activity was acquired on the EnSpire plate reader (PerkinElmer).

qPCR

Total RNA at days 0, 30, 45, and 60 of each of the line were reverse transcribed (Quantitech, Qiagen) and amplified material was detected using commercially available Taqman gene-expression assays (Applied Biosystems) with the data normalized to hypoxanthine phosphoribosyltransferase 1 (*HPRT*). Each data point represents nine technical replicates from three independent experiments.

Western Blotting

Neuronal cultures were scraped and proteins from cell pellets were extracted using 1% Triton X-100 extraction buffer as previously described (Mazzulli et al., 2011). Antibodies used for western blotting were anti-α-synuclein (Syn211, 1:1,000, Sigma; LB509, 1:500, Abcam; C20, 1:2,000, Santa Cruz Biotechnology), anti-βIII-tubulin (1:6,000, Sigma), and anti-glyceraldehyde 3-phosphate dehydrogenase (GAPDH, 1:5,000, Millipore). Detection was done using fluorescently labeled secondaries (Alexa 680 or IRDye 800), scanned and analyzed using the Odyssey infrared imaging system (LI-COR Biosciences). Integrated band intensities of α-synuclein or normalizing controls were quantified from three different culture sets. ANOVA with Tukey's post hoc test was used for statistical analysis (GraphPad Prism software).

DA Measurements

To measure the intracellular DA level, we manually lysed 65-day-old mDA neurons in PBS containing 1% Triton X-100 and 200 μM ascorbic acid (Sigma). After a 15-min spin, the supernatant was collected. From each sample, an aliquot was removed directly to measure protein concentration. The remaining amount was loaded for DA measurement by HPLC with electrochemical detection as previously described (Studer et al., 1996) or the Dopamine Research ELISA kit (LDN). Cells in each sample were collected to normalize for protein content. DA concentrations in each group of samples were normalized to the levels

in the corresponding control group; data are shown as averaged normalized values from six independent experiments (floor plate) and four technical replications from two independent experiments (MS5).

Lentiviral Induction

Human *PINK1-V5* cDNA were cloned into lentiviral *pER4* vectors containing a neuron-specific PGK promoter (Déglon et al., 2000). Virus production was conducted according to standard protocols. Cells were infected on day 35 of differentiation with an MOI of 1–5. Infection efficiencies of *PINK1-V5* virus (80%) were analyzed by immunostaining at 25 days post infection.

Quantification

The percentages of marker-positive cells at the FP (day 11), mDA neuron precursor (day 25), and mature DA neuron (day 50 or later) stages were determined in samples derived from at least three independent experiments. Images for quantification were selected in a uniform random manner and each image was scored first for the number of DAPI-positive nuclei, followed by counting the number of cells expressing the marker of interest. ImageJ was used for some cases of image quantification. All data are presented as mean ± SEM. Statistical analysis was performed using Student's t test (comparing two groups) or ANOVA with Dunnett's test (comparing multiple groups against control).

SUPPLEMENTAL INFORMATION

Supplemental Information includes Supplemental Experimental Procedures, six figures, and two tables and can be found with this article online at http://dx.doi.org/10.1016/j.stemcr.2016.08.012.

AUTHOR CONTRIBUTIONS

S.C. and S.K. designed and performed the experiments, analyzed the data, and wrote the manuscript. J.R.M., J.G., A.M., E.V.M., T.A.M., and T.T. contributed to experiments, discussed the results, and commented on the manuscript. L.P. and P.V. assisted in conducting experiments and analyzed data. D.S. and D.K. discussed the results and commented on the manuscript. L.S. designed the concept, and wrote and approved the manuscript. J.S. supervised the project, conceptualized the experiments, analyzed the data, and wrote the manuscript.

ACKNOWLEDGMENTS

We thank M. Tomishima (SKI stem cell core) for excellent technical support. J.S. was supported in part by a fellowship from the New York Stem Cell Foundation (NYSCF). The work was supported in part by grants from NIH/NINDS (RO1NS052671, U24NS078338) and the Starr Foundation to L.S., the National Research Foundation of Korea (NRF-2014R1A1A2057443), Global Research Development Center (NRF-2016K1A4A3914725), and Functional Districts of the Science Belt support program (2015K000278) to J.S., NIH/NINDS Grant R01NS092823 to J.R.M., and NIH grants HL098351, HL09571 and DA08259 to T.A.M., and also by P30 CA008748.

Received: December 21, 2015
Revised: August 17, 2016
Accepted: August 17, 2016
Published: September 15, 2016

REFERENCES

Abeliovich, A., Schmitz, Y., Farinas, I., Choi-Lundberg, D., Ho, W.H., Castillo, P.E., Shinsky, N., Verdugo, J.M., Armanini, M., Ryan, A., et al. (2000). Mice lacking alpha-synuclein display functional deficits in the nigrostriatal dopamine system. Neuron *25*, 239–252.

Arima, K., Ueda, K., Sunohara, N., Hirai, S., Izumiyama, Y., Tonozuka-Uehara, H., and Kawai, M. (1998). Immunoelectron-microscopic demonstration of NACP/alpha-synuclein-epitopes on the filamentous component of Lewy bodies in Parkinson's disease and in dementia with Lewy bodies. Brain Res. *808*, 93–100.

Baba, M., Nakajo, S., Tu, P.H., Tomita, T., Nakaya, K., Lee, V.M., Trojanowski, J.Q., and Iwatsubo, T. (1998). Aggregation of alpha-synuclein in Lewy bodies of sporadic Parkinson's disease and dementia with Lewy bodies. Am. J. Pathol. *152*, 879–884.

Bartels, T., Choi, J.G., and Selkoe, D.J. (2011). α-Synuclein occurs physiologically as a helically folded tetramer that resists aggregation. Nature *477*, 107–110.

Bellin, M., Marchetto, M.C., Gage, F.H., and Mummery, C.L. (2012). Induced pluripotent stem cells: the new patient? Nat. Rev. Mol. Cell Biol. *13*, 713–726.

Bellucci, A., Zaltieri, M., Navarria, L., Grigoletto, J., Missale, C., and Spano, P. (2012). From α-synuclein to synaptic dysfunctions: new insights into the pathophysiology of Parkinson's disease. Brain Res. *1476*, 183–202.

Bendor, J.T., Logan, T.P., and Edwards, R.H. (2013). The function of alpha-synuclein. Neuron *79*, 1044–1066.

Chambers, S.M., Fasano, C.A., Papapetrou, E.P., Tomishima, M., Sadelain, M., and Studer, L. (2009). Highly efficient neural conversion of human ES and iPS cells by dual inhibition of SMAD signaling. Nat. Biotechnol. *27*, 275–280.

Cooper, O., Seo, H., Andrabi, S., Guardia-Laguarta, C., Graziotto, J., Sundberg, M., McLean, J.R., Carrillo-Reid, L., Xie, Z., Osborn, T., et al. (2012). Pharmacological rescue of mitochondrial deficits in iPSC-derived neural cells from patients with familial Parkinson's disease. Sci. Transl. Med. *4*, 141ra190.

Davidson, W.S., Jonas, A., Clayton, D.F., and George, J.M. (1998). Stabilization of alpha-synuclein secondary structure upon binding to synthetic membranes. J. Biol. Chem. *273*, 9443–9449.

Dawson, T.M., Ko, H.S., and Dawson, V.L. (2010). Genetic animal models of Parkinson's disease. Neuron *66*, 646–661.

Déglon, N., Tseng, J.L., Bensadoun, J.C., Zurn, A.D., Arsenijevic, Y., Pereira de Almeida, L., Zufferey, R., Trono, D., and Aebischer, P. (2000). Self-inactivating lentiviral vectors with enhanced transgene expression as potential gene transfer system in Parkinson's disease. Hum. Gene Ther. *11*, 179–190.

Deng, H., Dodson, M.W., Huang, H., and Guo, M. (2008). The Parkinson's disease genes pink1 and parkin promote mitochondrial

fission and/or inhibit fusion in Drosophila. Proc. Natl. Acad. Sci. USA *105*, 14503–14508.

Devi, L., Raghavendran, V., Prabhu, B.M., Avadhani, N.G., and Anandatheerthavarada, H.K. (2008). Mitochondrial import and accumulation of alpha-synuclein impair complex I in human dopaminergic neuronal cultures and Parkinson disease brain. J. Biol. Chem. *283*, 9089–9100.

Devine, M.J., Ryten, M., Vodicka, P., Thomson, A.J., Burdon, T., Houlden, H., Cavaleri, F., Nagano, M., Drummond, N.J., Taanman, J.W., et al. (2011). Parkinson's disease induced pluripotent stem cells with triplication of the alpha-synuclein locus. Nat. Commun. *2*, 440.

Engelender, S. (2008). Ubiquitination of alpha-synuclein and autophagy in Parkinson's disease. Autophagy *4*, 372–374.

Exner, N., Treske, B., Paquet, D., Holmström, K., Schiesling, C., Gispert, S., Carballo-Carbajal, I., Berg, D., Hoepken, H.H., Gasser, T., et al. (2007). Loss-of-function of human PINK1 results in mitochondrial pathology and can be rescued by parkin. J. Neurosci. *27*, 12413–12418.

Farrer, M., Chan, P., Chen, R., Tan, L., Lincoln, S., Hernandez, D., Forno, L., Gwinn-Hardy, K., Petrucelli, L., Hussey, J., et al. (2001). Lewy bodies and parkinsonism in families with parkin mutations. Ann. Neurol. *50*, 293–300.

Gaugler, M.N., Genc, O., Bobela, W., Mohanna, S., Ardah, M.T., El-Agnaf, O.M., Cantoni, M., Bensadoun, J.C., Schneggenburger, R., Knott, G.W., et al. (2012). Nigrostriatal overabundance of alpha-synuclein leads to decreased vesicle density and deficits in dopamine release that correlate with reduced motor activity. Acta Neuropathol. *123*, 653–669.

Giasson, B.I., Duda, J.E., Murray, I.V., Chen, Q., Souza, J.M., Hurtig, H.I., Ischiropoulos, H., Trojanowski, J.Q., and Lee, V.M. (2000). Oxidative damage linked to neurodegeneration by selective alpha-synuclein nitration in synucleinopathy lesions. Science *290*, 985–989.

Hauser, D.N., and Hastings, T.G. (2013). Mitochondrial dysfunction and oxidative stress in Parkinson's disease and monogenic parkinsonism. Neurobiol. Dis. *51*, 35–42.

Imaizumi, Y., Okada, Y., Akamatsu, W., Koike, M., Kuzumaki, N., Hayakawa, H., Nihira, T., Kobayashi, T., Ohyama, M., Sato, S., et al. (2012). Mitochondrial dysfunction associated with increased oxidative stress and alpha-synuclein accumulation in PARK2 iPSC-derived neurons and postmortem brain tissue. Mol. Brain *5*, 35.

Jiang, H., Ren, Y., Yuen, E.Y., Zhong, P., Ghaedi, M., Hu, Z., Azabdaftari, G., Nakaso, K., Yan, Z., and Feng, J. (2012). Parkin controls dopamine utilization in human midbrain dopaminergic neurons derived from induced pluripotent stem cells. Nat. Commun. *3*, 668.

Keeney, P.M., Xie, J., Capaldi, R.A., and Bennett, J.P. (2006). Parkinson's disease brain mitochondrial complex I has oxidatively damaged subunits and is functionally impaired and misassembled. J. Neurosci. *26*, 5256–5264.

Kim, H., Lee, G., Ganat, Y., Papapetrou, E.P., Lipchina, I., Socci, N.D., Sadelain, M., and Studer, L. (2011). miR-371-3 expression predicts neural differentiation propensity in human pluripotent stem cells. Cell Stem Cell *8*, 695–706.

Kitada, T., Asakawa, S., Hattori, N., Matsumine, H., Yamamura, Y., Minoshima, S., Yokochi, M., Mizuno, Y., and Shimizu, N. (1998). Mutations in the parkin gene cause autosomal recessive juvenile parkinsonism. Nature *392*, 605–608.

Klein, C., and Schlossmacher, M.G. (2006). The genetics of Parkinson disease: implications for neurological care. Nat. Clin. Pract. Neurol. *2*, 136–146.

Kriks, S., Shim, J.W., Piao, J., Ganat, Y.M., Wakeman, D.R., Xie, Z., Carrillo-Reid, L., Auyeung, G., Antonacci, C., Buch, A., et al. (2011). Dopamine neurons derived from human ES cells efficiently engraft in animal models of Parkinson's disease. Nature *480*, 547–551.

Lesage, S., and Brice, A. (2009). Parkinson's disease: from monogenic forms to genetic susceptibility factors. Hum. Mol. Genet. *18*, R48–R59.

Marques, O., and Outeiro, T.F. (2012). Alpha-synuclein: from secretion to dysfunction and death. Cell Death Dis. *3*, e350.

Mazzulli, J.R., Xu, Y.H., Sun, Y., Knight, A.L., McLean, P.J., Caldwell, G.A., Sidransky, E., Grabowski, G.A., and Krainc, D. (2011). Gaucher disease glucocerebrosidase and alpha-synuclein form a bidirectional pathogenic loop in synucleinopathies. Cell *146*, 37–52.

Mazzulli, J.R., Zunke, F., Isacson, O., Studer, L., and Krainc, D. (2016). alpha-Synuclein-induced lysosomal dysfunction occurs through disruptions in protein trafficking in human midbrain synucleinopathy models. Proc. Natl. Acad. Sci. USA *113*, 1931–1936.

Miller, J.D., Ganat, Y.M., Kishinevsky, S., Bowman, R.L., Liu, B., Tu, E.Y., Mandal, P.K., Vera, E., Shim, J.W., Kriks, S., et al. (2013). Human iPSC-based modeling of late-onset disease via progerin-induced aging. Cell Stem Cell *13*, 691–705.

Milner, T.A., Waters, E.M., Robinson, D.C., and Pierce, J.P. (2011). Degenerating processes identified by electron microscopic immunocytochemical methods. Methods Mol. Biol. *793*, 23–59.

Mosharov, E.V., Staal, R.G., Bove, J., Prou, D., Hananiya, A., Markov, D., Poulsen, N., Larsen, K.E., Moore, C.M., Troyer, M.D., et al. (2006). Alpha-synuclein overexpression increases cytosolic catecholamine concentration. J. Neurosci. *26*, 9304–9311.

Mosharov, E.V., Larsen, K.E., Kanter, E., Phillips, K.A., Wilson, K., Schmitz, Y., Krantz, D.E., Kobayashi, K., Edwards, R.H., and Sulzer, D. (2009). Interplay between cytosolic dopamine, calcium, and alpha-synuclein causes selective death of substantia nigra neurons. Neuron *62*, 218–229.

Murphy, D.D., Rueter, S.M., Trojanowski, J.Q., and Lee, V.M. (2000). Synucleins are developmentally expressed, and alpha-synuclein regulates the size of the presynaptic vesicular pool in primary hippocampal neurons. J. Neurosci. *20*, 3214–3220.

Narendra, D.P., Jin, S.M., Tanaka, A., Suen, D.F., Gautier, C.A., Shen, J., Cookson, M.R., and Youle, R.J. (2010). PINK1 is selectively stabilized on impaired mitochondria to activate Parkin. PLoS Biol. *8*, e1000298.

Nemani, V.M., Lu, W., Berge, V., Nakamura, K., Onoa, B., Lee, M.K., Chaudhry, F.A., Nicoll, R.A., and Edwards, R.H. (2010). Increased expression of alpha-synuclein reduces neurotransmitter release

by inhibiting synaptic vesicle reclustering after endocytosis. Neuron *65*, 66–79.

Nguyen, H.N., Byers, B., Cord, B., Shcheglovitov, A., Byrne, J., Gujar, P., Kee, K., Schule, B., Dolmetsch, R.E., Langston, W., et al. (2011). LRRK2 mutant iPSC-derived DA neurons demonstrate increased susceptibility to oxidative stress. Cell Stem Cell *8*, 267–280.

Norris, E.H., Uryu, K., Leight, S., Giasson, B.I., Trojanowski, J.Q., and Lee, V.M. (2007). Pesticide exposure exacerbates alpha-synucleinopathy in an A53T transgenic mouse model. Am. J. Pathol. *170*, 658–666.

Paxinou, E., Chen, Q., Weisse, M., Giasson, B.I., Norris, E.H., Rueter, S.M., Trojanowski, J.Q., Lee, V.M., and Ischiropoulos, H. (2001). Induction of alpha-synuclein aggregation by intracellular nitrative insult. J. Neurosci. *21*, 8053–8061.

Perrier, A.L., Tabar, V., Barberi, T., Rubio, M.E., Bruses, J., Topf, N., Harrison, N.L., and Studer, L. (2004). Derivation of midbrain dopamine neurons from human embryonic stem cells. Proc. Natl. Acad. Sci. USA *101*, 12543–12548.

Peters, A., Palay, S., and Webster, H. (1991). The Fine Structure of the Nervous System (Oxford University Press).

Pickrell, A.M., and Youle, R.J. (2008). The roles of PINK1, Parkin, and mitochondrial fidelity in Parkinson's disease. Neuron *85*, 257–273.

Platt, N.J., Gispert, S., Auburger, G., and Cragg, S.J. (2012). Striatal dopamine transmission is subtly modified in human A53Tα-synuclein overexpressing mice. PLoS One *7*, e36397.

Poole, A.C., Thomas, R.E., Andrews, L.A., McBride, H.M., Whitworth, A.J., and Pallanck, L.J. (2008). The PINK1/Parkin pathway regulates mitochondrial morphology. Proc. Natl. Acad. Sci. USA *105*, 1638–1643.

Seibler, P., Graziotto, J., Jeong, H., Simunovic, F., Klein, C., and Krainc, D. (2011). Mitochondrial Parkin recruitment is impaired in neurons derived from mutant PINK1 iPS cells. J. Neurosci. *31*, 5970–5976.

Shaltouki, A., Sivapatham, R., Pei, Y., Gerencser, A.A., Momčilović, O., Rao, M.S., and Zeng, X. (2015). Mitochondrial alterations by PARKIN in dopaminergic neurons using PARK2 patient-specific and PARK2 knockout isogenic iPSC lines. Stem Cell Rep. *4*, 847–859.

Sherer, T.B., Betarbet, R., Stout, A.K., Lund, S., Baptista, M., Panov, A.V., Cookson, M.R., and Greenamyre, J.T. (2002). An in vitro model of Parkinson's disease: linking mitochondrial impairment to altered alpha-synuclein metabolism and oxidative damage. J. Neurosci. *22*, 7006–7015.

Studer, L., Psylla, M., Bühler, B., Evtouchenko, L., Vouga, C., Leenders, K., Seiler, R., and Spenger, C. (1996). Noninvasive dopamine determination by reversed phase HPLC in the medium of free-floating roller tube cultures of rat fetal ventral mesencephalon: a tool to assess dopaminergic tissue prior to grafting. Brain Res. Bull. *41*, 143–150.

Valente, E.M., Abou-Sleiman, P.M., Caputo, V., Muqit, M.M., Harvey, K., Gispert, S., Ali, Z., Del Turco, D., Bentivoglio, A.R., Healy, D.G., et al. (2004). Hereditary early-onset Parkinson's disease caused by mutations in PINK1. Science *304*, 1158–1160.

Woods, W.S., Boettcher, J.M., Zhou, D.H., Kloepper, K.D., Hartman, K.L., Ladror, D.T., Qi, Z., Rienstra, C.M., and George, J.M. (2007). Conformation-specific binding of alpha-synuclein to novel protein partners detected by phage display and NMR spectroscopy. J. Biol. Chem. *282*, 34555–34567.

Yavich, L., Tanila, H., Vepsalainen, S., and Jakala, P. (2004). Role of alpha-synuclein in presynaptic dopamine recruitment. J. Neurosci. *24*, 11165–11170.

Zaltieri, M., Grigoletto, J., Longhena, F., Navarria, L., Favero, G., Castrezzati, S., Colivicchi, M.A., Della Corte, L., Rezzani, R., Pizzi, M., et al. (2015). alpha-synuclein and synapsin III cooperatively regulate synaptic function in dopamine neurons. J. Cell Sci. *128*, 2231–2243.